Molecular Design of DNA-Directed Ligands with Specific Interactions: Solution NMR Studies of the Interaction of a *m*-Hydroxy Analogue of Hoechst 33258 with d(CGCGAATTCGCG)$_2$

John A. Parkinson,‡ Seyed E. Ebrahimi,§ James H. McKie,§ and Kenneth T. Douglas*,§

Department of Pharmacy, University of Manchester, Manchester M13 9PL, U.K., and Department of Chemistry, University of Edinburgh, West Mains Road, Edinburgh EH9 3JJ, U.K.

Received December 22, 1993; Revised Manuscript Received April 27, 1994®

ABSTRACT: We have used one-dimensional (1D) and two-dimensional (2D) proton nuclear magnetic resonance spectroscopy at 600 MHz for structural analysis of the complex formed between d(CGCGAATTCGCG)$_2$ and 2-[2-(3-hydroxyphenyl)-6-benzimidazoyl]-6-(1-methyl-4-piperazinyl)benzimidazole (*meta*-Hoechst). This analogue differs from Hoechst 33258 only in the location of its *meta* rather than *para* phenolic hydroxyl group and was designed to introduce the possibility of intermolecular hydrogen bonding to DNA via the phenol. Complex formation was shown to be 1:1 at 25 °C in phosphate buffer in D_2O by 1D NMR spectroscopic titration of a solution of d(CGCGAATTCGCG)$_2$ with *meta*-Hoechst. From 1D NMR spectroscopy the observed perturbations of the assigned chemical shifts of the oligonucleotide observed on binding *meta*-Hoechst could be used to locate the ligand in the central AATT stretch. By means of 2D NMR spectroscopic techniques, over 400 proton–proton NOEs were defined within the complex. DNA nonexchangeable resonance assignments were made using the sequential assignment method and NOESY. Binding the unsymmetrical ligand lifted the C_{2v} symmetry of the DNA. Exchangeable hydrogens were assigned from NOESY data acquired in 85% H_2O/15% D_2O medium for the complex and showed differences between the Hoechst 33258 and *meta*-Hoechst complexes with d(CGCGAATTCGCG)$_2$. The location of *meta*-Hoechst in the minor-groove AATT region was triangulated using 32 intermolecular NOEs determined for the complex. From the intermolecular NOEs involving the aromatic C–H protons of the phenolic ring of *meta*-Hoechst, it was clear that this region of the molecule did not rotate freely within the minor groove on the NMR time scale and was oriented with its hydroxyl group toward the floor of the minor groove, in line with the occurrence of the predicted hydrogen bonding between it and the DNA. The pK_a of the N3H proton of *meta*-Hoechst in its bound state in this complex was measured as 6.1 by NMR spectroscopy, a value slightly elevated relative to estimates (~5.2) of the pK_a of this proton for the free ligand. Molecular mechanics and the distance restraints provided by the intermolecular NOEs were used in molecular modeling of the *meta*-Hoechst/d(CGCGAATTCGCG)$_2$ complex, and the distances in the model were consistent with the formation of hydrogen bonds involving the *m*-OH group of *meta*-Hoechst and the DNA.

In principle, drugs might be designed on the basis of DNA sequence recognition, although to pinpoint a unique target in the human genome, with base sequence as their only guide, would require recognition of about 15–16 base pairs (Toulme & Hélène, 1988). A more realistic target may be to attack DNA in the process of undergoing enzymatic processing, and recently some minor-groove binders have been found to inhibit topoisomerase activity in whole cells (Beerman et al., 1992; Sing et al., 1992). At a chemical level, the design of sequence-specific minor-groove ligands presents several challenges. Whatever the free solution conformation of the ligand, it must be able to adapt its shape to track closely the contours of the helical minor-groove valley. Added to this, its charge distribution must remain appropriate for the minor groove, whose electrostatic potential changes according to base sequence (Bontemps et al., 1975).

The discovery of the details of minor-groove binding of the natural antibiotics distamycin and netropsin (Kopka et al., 1985; Lown et al., 1977) spawned the emergence of synthetic sequence-reading molecules based on them, the lexitropsins (Kopka et al., 1985) and the isolexins (Goodsell & Dickerson, 1986). Recently, the fluorescent histochemical stain (Latt & Stetten, 1976) Hoechst 33258 (**1**) has emerged as a model for

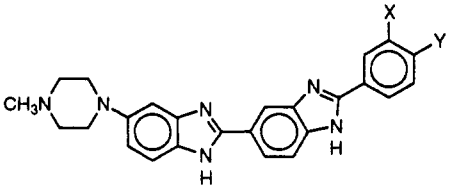

Hoechst 33258 (1; X = H, Y = OH)
meta-Hoechst (2; X = OH, Y = H)
Hoechst 33342 (3; X = H, Y = OEt)

minor-groove ligand design (Bathini et al., 1990; Rao & Lown, 1991; Ebrahimi et al., 1992). As a drug progenitor, Hoechst 33258 has a number of useful features. It binds strongly and selectively to double-stranded DNA but not to double-stranded RNA, A-DNA, nor any other non-B-DNA structure (Muller

* To whom correspondence should be addressed.
‡ University of Edinburgh.
§ University of Manchester.
® Abstract published in *Advance ACS Abstracts,* June 15, 1994.
[1] Abbreviations: DQFCOSY, double quantum filtered two-dimensional homonuclear correlation spectroscopy; NOESY, two-dimensional nuclear Overhauser enhancement spectroscopy; ROESY, rotating frame two-dimensional Overhauser enhancement spectroscopy; TOCSY, two-dimensional total correlation spectroscopy; TSP, sodium 3-(trimethylsilyl)-2,2,3,3-$^2H_4$)-1-propionate; *meta*-Hoechst, 2-[2-(3-hydroxyphenyl)-6-benzimidazolyl]-6-(1-methyl-4-piperazinyl)benzimidazole.

0006-2960/94/0433-8442$04.50/0

& Gautier, 1975). It is readily taken up by cells (Muller & Gautier, 1975; Bontemps et al., 1975; Comings, 1975; Steiner & Sternberg, 1979; Mikailor et al., 1981; Zimmer & Wahnert, 1986) although there are indications that there may already be a means of molecular cell resistance to such minor-groove drugs (Smith et al., 1988), as a mouse cell-line has been derived which is 30 times more resistant than the parental line to Hoechst 33342 (3) because of increased ability of the daughter cell-line to dissociate the dye/DNA complex (Smith et al., 1988).

The binding of Hoechst 33258 to B-DNA has been studied in detail by X-ray diffraction (Sriram et al., 1992; Carrondo et al., 1989; Teng et al., 1986; Pjura et al., 1987; Quintana et al., 1991), NMR spectroscopy (Kumar et al., 1992; Fede et al., 1991; Parkinson et al., 1990, 1992; Searle & Embrey, 1990; Kumar et al., 1990; Embrey et al., 1991), fluorescence spectroscopy (Loontiens et al., 1990, 1991; Härd et al., 1990; Jin & Breslauer, 1988), and a range of other biophysical techniques (Bathini et al., 1990) including molecular mechanical calculations (Haworth et al., 1991). The chemistry of molecular recognition has been approached by altering both the base structure of the target DNA (Carrondo et al., 1989; Embrey et al., 1991; Loontiens et al., 1990, 1991) and the structure of the Hoechst molecule (Bathini et al., 1990; Kumar et al., 1992; Sriram et al., 1992; Ebrahimi et al., 1992). The nature of the DNA sequence is important, as in the crystalline complexes of Hoechst 33258 with $d(CGCGAATTCGCG)_2$ (Teng et al., 1986; Pjura et al., 1987; Quintana et al., 1991) and the closely similar $d(CGCGATATCGCG)_2$ (Carrondo et al., 1989) the *orientations* of the ligand along the minor groove are actually opposite. This orientation problem, a feature of the crystalline structure of the DNA (Quintana et al., 1991), does not appear to arise in solution on the basis of detailed NMR studies (Parkinson et al., 1990, 1992). From our previous NMR studies we were struck by the wealth of intermolecular NOEs in the NOESY spectrum of **1** bound to $d(CGCGAATTCGCG)_2$ (Parkinson et al., 1990), an experimental handle which allows the precise triangulation of the binding site and conformation of Hoechst 33258 or its derivatives bound to this duplex. Work from a range of laboratories has now shown that the DNA binding of Hoechst 33258, driven to AT-rich regions, is extremely tight, a dissociation constant of 3 nM having been determined carefully for **1** with $d(CCGGAATTCGCG)_2$ (Loontiens et al., 1990).

To date, most reported structural variations of the Hoechst 33258 structure have been aimed at compromising the AT selectivity to allow a measure of G-C recognition (Sriram et al., 1992; Rao et al., 1990; Bathini et al., 1990), using chemical changes within one or both of the benzimidazole systems. We have chosen, in a complementary approach capitalizing on the strongly AT-directing nature of the Hoechst 33258 molecular architecture, to use the Hoechst 33258 structure as a molecular anchor, tightly sealing the ligand to an AATT (or similar) patch on DNA, and to add additional sequence-determining features to the ends of the molecule. Although in enzymology the field of active-site-directed inhibitor design is well-advanced, it is less so for DNA. One feature that is clear from rational enzyme inhibitor design is that attempting to structurally modify a lead enzyme inhibitor to incorporate too many new potential binding sites usually results in a compromise once the binding of the new inhibitor has been determined. Even a small change between two molecules can result in quite a major difference in the way in which they reside physically within an active site. Experience in rationally designing DNA-directed ligands is considerably less advanced than that in enzymology.

Chart 1: Nomenclature

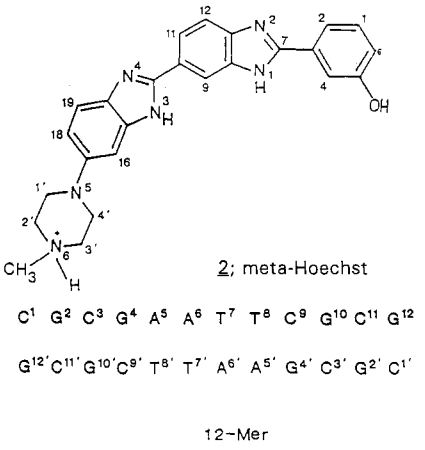

Our computer graphics analysis of the structural model of the Hoechst 33258/$d(CGCGAATTCGCG)_2$ complex, which we derived from NMR spectroscopic studies, provided an opportunity to probe the predictability (or otherwise) of designed interactions in DNA/minor-groove ligand complex design. We predicted that merely moving the phenolic OH group of Hoechst 33258 (**1**) from the *para* to the *meta* position (to give *meta*-Hoechst, **2**) would lead to additional putative hydrogen bonding from the *m*-OH group of **2** to the C=O group of C^9 and the NH_2 group of $G^{4'}$ (Ebrahimi et al., 1992). We now provide details of the binding of **2** to $d(CGCGAATTCGCG)_2$ as determined by NMR spectroscopy.

MATERIALS AND METHODS

Sample Preparation for NMR Spectroscopy. A gift of $d(CGCGAATTCGCG)_2$, from the Oswell DNA unit (University of Edinburgh) was prepared for NMR experiments by dissolving it (8.5 mg) in buffer (0.5 mL of 100 mM NaCl, 10 mM NaH_2PO_4, 1 mM TSP, and 0.1 mM NaN_3 prepared in 99.8% D_2O). The pH of the sample was adjusted to 7.00, and the sample was lyophilized and resuspended in 99.8% D_2O (0.5 mL). A 1:1 mixture of DNA and *meta*-Hoechst was produced by stepwise addition of aliquots of *meta*-Hoechst (1.01 mg in 10 μL) in D_2O to the DNA solution, observing the subsequent ^1H NMR spectrum of each mixture. A 1:1 complex was observed to have formed when resonances from the free oligonucleotide had been completely replaced by resonances from the complex, the appearance of which was similar to that from a previous study of Hoechst 33258 (*para*-Hoechst) bound to the same oligonucleotide (Parkinson et al., 1990). Following addition of ligand, the sample pH was measured as 7.46 (=pH_{meas}, uncorrected meter reading). The synthesis of *meta*-Hoechst will be described elsewhere.

Nomenclature. The atom labeling of *meta*-Hoechst (**2**) and the duplex of $d(CGCGAATTCGCG)_2$ used in this study is shown in Chart 1.

NMR Experiments. NMR data were collected on a Varian VXR 600S NMR spectrometer operating at a proton resonance frequency of 599.945 MHz and equipped with a Sun 4/110 host computer running VNMR system software version 3.2. A dedicated proton probe head was used for all proton observations. Sets of data were collected for the free oligonucleotide and for the complex.

Pure absorption two-dimensional DQF COSY (Piantini et al., 1982; Rance et al., 1983), TOCSY (Bax & Davis, 1985), ROESY (Kessler et al., 1989), and NOESY (Nagayama et

Table 1: *meta*-Hoechst Resonance Assignments in Its 1:1 Complex with d(CGCGAATTCGCG)$_2$ Measured at 600 MHz[a]

MH1	7.615 (t)	MH9 8.145 (s)	MH16	7.407 (s)	MHCH3	2.967 (s)
MH2	7.950 (d)	MH11 7.961 (d)	MH18	7.197 (d)	MHO*H*[b]	13.17
MH4	7.335 (s)	MH12 8.261 (d)	MH19	7.735 (d)		
MH6	7.107 (d)		MHN3H	11.369 (s)		

[a] See text for details of method and sample conditions: (s) singlet, (d) = doublet, (t) = triplet. [b] Broad lump at pH = 5.40; speculative assignment only based on NOE to MH4.

Table 2: Assignment of DNA ^{1}H Resonances at 600 MHz in the 1:1 *meta*-Hoechst Complex with d(CGCGAATTCGCG)$_2$[a]

												amino		imino	
	C2H	C8H	C6H	CH_3	C5H	C1′	C2′H	C2″H	C3′H	C4′H	C5′H	C5″H	N4H(1)	N4H(2)	N1H	N3H
C^1			7.609		5.900	5.745	1.923	2.392	4.688	4.062	3.71	3.71				
G^2		7.929				5.860	2.625	2.685	4.961	4.336	4.08	3.97			13.025	
C^3			7.228		5.362	5.700	1.713	2.190	4.800	4.141	N.A.	N.A.	6.410	8.380		
G^4		7.802				5.070	2.600	2.600	4.961	4.238	4.06	3.94			12.900	
A^5	7.491	8.282				5.840	2.870	2.914	5.113	4.444	4.18	4.10				
A^6	8.269	8.276				6.227	2.748	2.748	5.084	4.050	N.A.	N.A.				
T^7			6.992	1.351		5.380	1.590	2.025	4.473	2.900	3.98	3.98				13.840
T^8			6.933	1.435		4.908	1.664	2.065	4.492	3.173	3.94	3.94				13.750
C^9			6.940		5.299	4.908	1.468	1.849	4.580	3.657	3.94	3.395	6.370	8.120		
G^{10}		7.760				5.810	2.611	2.655	4.975	4.390	N.A.	N.A.			12.820	
C^{11}			7.292		5.381	5.750	1.890	2.333	4.820	4.175	N.A.	N.A.	6.540	8.430		
G^{12}		7.929				6.155	2.385	2.619	4.678	4.175	N.A.	N.A.				
C$^{1'}$			7.594		5.879	5.745	1.923	2.392	4.688	4.062	3.71	3.71				
G$^{2'}$		7.915				5.860	2.625	2.685	4.961	4.336	4.08	3.97			13.010	
C$^{3'}$			7.252		5.350	5.545	1.796	2.255	4.790	4.106	N.A.	N.A.	6.400	8.420		
G$^{4'}$		7.861				5.643	2.709	2.875	5.025	4.337	N.A.	N.A.			12.880	
A$^{5'}$	7.802	8.083				6.155	2.619	2.978	5.074	4.522	4.24	4.24				
A$^{6'}$	8.452	8.140				5.730	2.300	2.621	4.771	4.510	N.A.	N.A.				
T$^{7'}$			6.826	1.252		5.260	1.510	2.030	4.390	3.706	N.A.	N.A.				13.830
T$^{8'}$			6.896	1.410		5.050	1.571	1.854	4.448	2.318	3.94	3.36				13.750
C$^{9'}$			7.380		5.567	5.325	2.100	2.280	4.810	4.238	N.A.	N.A.	6.760	8.540		
G$^{10'}$		7.888				5.906	2.650	2.730	5.010	4.390	N.A.	N.A.			13.000	
C$^{11'}$			7.326		5.471	5.770	1.890	2.333	4.815	4.150	N.A.	N.A.	6.600	8.460		
G$^{12'}$		7.929				6.155	2.385	2.619	4.678	4.175	N.A.	N.A.				

[a] Nonexchangeable hydrogen resonances were assigned from data recorded at 30 °C. Exchangeable hydrogen resonances are for data collected at 25 °C. Shifts are in parts per million to high frequency relative to the methyl singlet of TSP at 0 ppm.

al., 1980; Jeener et al., 1979; Macura et al., 1981) data were collected with quadrature detection into 4096 complex data points for 2 × 256 t_1 increments in the hypercomplex phase-sensitive mode (States et al., 1982); 40 transients were acquired for each t_1 increment. The residual *H*OD resonance was suppressed by continuous, low-power irradiation during the recycle time of 2 s. In the NOESY experiment, solvent suppression was achieved by low-power irradiation during the recycle and mixing times. Data were acquired over a 6-kHz spectral width to give a final ω_2 digital resolution of 1.46 Hz point^{-1}. NOESY data were acquired with mixing times of 50, 95, 150, 200, and 300 ms at 20, 25, 30, and 36 °C. TOCSY data were acquired with a mixing time of 80 ms. ROESY data were acquired at 30 °C with mixing times of 75 and 150 ms. All two-dimensional data sets were acquired nonspinning in an interleaved fashion to reduce t_1 noise and other artifacts.

One-dimensional ^{1}H NMR spectra of the complex dissolved in 99.8% D_2O were acquired between 9 and 36 °C. Data were collected into 32K data points over a spectral width of 6 kHz; for each spectrum 128 transients were acquired with a 3-s recycle delay during which the residual *H*OD resonance was suppressed by continuous low-power irradiation.

Pure absorption two-dimensional NOESY data were accumulated on the complex dissolved in 85% H_2O/15% D_2O and collected with quadrature detection into 4056 complex data points for 2 × 256 t_1 increments in the hypercomplex phase-sensitive mode (States et al., 1982); 64 transients were required for each free induction decay. A nonexcitation water suppression technique was used to eliminate the solvent resonance in which the final pulse of the NOESY experiment was replaced by a symmetrically shifted read pulse calibrated to provide maximum excitation in the region of interest. A 1.5-s recycle delay and a 175-ms mixing time served as the fixed delay periods in the pulse scheme. Data was acquired over a 14-kHz spectral width.

One-dimensional data acquisitions on the sample in 85% H_2O/15% D_2O, carried out at 7, 8, 12, 15 and 20 °C, were collected into 32K data points over a spectral width of 13 kHz; 128 transients were accumulated with a presaturation period of 2 s. A nonexcitation water suppression scheme was also used to accumulate data on the sample under these solvent conditions at 25 °C in which the first increment of a NOESY pulse scheme containing a symmetrically shifted read pulse was achieved by linear prediction to correct for phase shifts introduced by the read pulse. Data acquired over a 14-kHz spectral width were collected into 70K data points.

All data were transferred to a remote Sun 4/330GX data station for processing using VNMR 3.2 software. 2D data sets were transformed by zero filling in ω_1 to 2048 data points before apodization in both dimensions prior to Fourier transformation. One-dimensional spectra were transformed after zero filling to 65K data points. Transformation of data acquired using pulse schemes possessing a symmetrically shifted read pulse was achieved by linear prediction to correct for phase shifts introduced by the read pulse, resulting in in-phase spectra of one sign across the entire sweep width. Both 1D and 2D data sets in both 99.8% D_2O and 85% H_2O/15% D_2O were referenced internally to the singlet methyl resonance of TSP at 0 ppm.

Molecular Modeling. A Silicon Graphics 240X Pathfinder workstation was used running QUANTA and CHARMM. Two models of the complex were generated. The first used only the three precisely determined NOE distances (MH4 to A5′2H, MH9 to A6′2H, and MH16 to A62H, 2.78, 2.66, and 2.86 Å, respectively). The ligand was graphically docked using QUANTA to meet the NOE distance constraints. Then, using atomic constraints to hold the B-DNA structure fully rigid, the ligand/DNA complex was minimized (500 iterations of ABNR). The second method employed the full set of constraints, the three distances above, and the additional 29 values (Table 3), which were all set to 4.00 Å with 0.5-Å boundary values to allow the distances to vary without too high a penalty (using QUANTA's CHARMM application to run the 'Distance Constraints' menu). Initially the *meta*-Hoechst was placed in the location equivalent to that for the NMR-derived *para*-Hoechst model (Parkinson et al., 1990). The complex was then minimized (500 iterations ABNR) with the 32 NOE distance constraints and atomic constraints employed to hold the B-DNA structure rigid. This was followed by minimization (500 iterations ABNR) in which the distance constraints were excluded but with the B-DNA atomic contraints still in effect. The first step was repeated (500 iterations ABNR) with both the distance and atomic constraints included. The final step (200 iterations of ABNR) did not use distance contraints but maintained the atomic constraints on the DNA. All calculations were run at 300 K *in vacuo* with a CHARMM constraints scale factor of 1.0.

Data Analysis. Analysis of pH-dependent data was carried out by least squares nonlinear regression analysis using the Enzfitter program, written by E. J. Leatherbarrow and distributed by Elsevier Biosoft.

RESULTS

Assignment of ^{1}H NMR Resonances in the Complex

Nonexchangeable Hydrogens. Data recorded on a sample of the 1:1 complex dissolved in 99.8% D_2O were assigned by combined use of TOCSY, DQFCOSY, and NOESY data sets. In all it was possible to define over 400 proton–proton NOEs for the complex. The aromatic hydrogen resonances of the bound *meta*-Hoechst ligand were readily observed in the TOCSY and DQFCOSY data sets, the aromatic to aromatic hydrogen cross-peak region of these types of data being relatively free of DNA cross-peak resonances. Thus it was possible to observe the three separate spin systems corresponding to nonexchangeable hydrogen atoms of two distinct benzimidazole moieties and the phenol moiety. Peak assignments for bound *meta*-Hoechst are shown in Table 1.

DNA hydrogen resonances were assigned using the sequential assignment method (Hare et al., 1983). The sugar 1′H to aromatic proton cross-peak region of the 250-ms NOESY spectrum at 30 °C is shown in Figure 1. The solid line maps the 'walk' from C^1 to G^{12} along one of the dNA strands. The dashed line maps the 'walk' from $C^{1'}$ to $G^{12'}$ on the complementary strand. The two strands of DNA have the same identity at either end but diverge from their second base-pair position onward through the region where the *meta*-Hoechst ligand is bound at the AATT site. The unsymmetrical ligand confers disymmetry on the self-complementary DNA, which usually has C_{2v} symmetry in the absence of any ligand. Some of the *meta*-Hoechst/DNA intermolecular NOEs are indicated by boxes in Figure 1.

The assignments of the resonances of the nonexchangeable hydrogen atoms in the DNA at 30 °C, shown in Table 2,

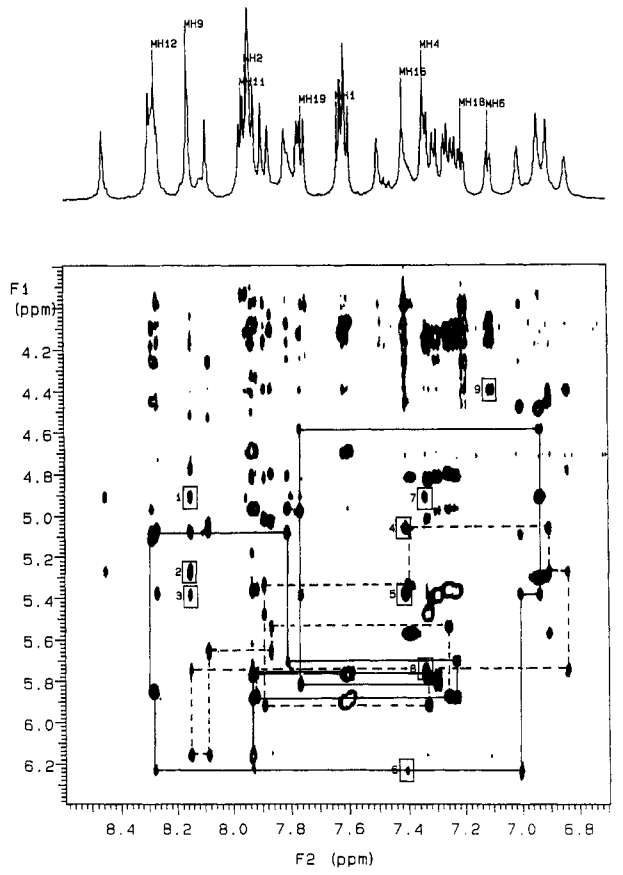

FIGURE 1: Aromatic to sugar 1′H region of the ^{1}H 250-ms NOESY spectrum of the 1:1 *meta*-Hoechst/d(CGCGAATTCGCG)$_2$ complex in 99% D_2O, 100 mM NaCl, 10 mM NaH_2PO_4, 1 mM TSP, data collected at 600 MHz. The solid line indicates the walk along one of the DNA strands between sugar 1′H resonances and base aromatic resonances. The dashed line corresponds to the same walk on the complementary strand. The strands are inequivalent due to the tight binding of the nonsymmetrical *meta*-Hoechst ligand. Assignments of the *meta*-Hoechst aromatic proton resonances are shown under the projection at the top of the figure. Boxed cross-peaks indicate some of the 32 assigned intermolecular NOEs between DNA and ligand, as detailed below: (1) MH9H–$T^8$1′H; (2) MH9H–$T^{7'}$1′H; (3) MH9H–$T^7$1′H; (4) MH16H–$T^{8'}$1′H; (5) MH16H–$T^7$1′H; (6) MH16H–$A^6$1′H; (7) MH4H–$T^8$1′H; (8) MH4H–$A^6$1′H; (9) MH6H–G^{10}4′H.

include a full set of assignments for the 4′H resonances. These proved elusive in the 500-MHz study of the *para*-Hoechst/d(CGCGAATTCGCG)$_2$ complex (Parkinson et al., 1990), and their complete identification here is important for two reasons. Firstly, they nullify assignments for the *para*-Hoechst piperazine ring nonexchangeable hydrogens derived from NMR data on the *para*-Hoechst/DNA complex (Parkinson et al., 1990). In the present case it has not been possible to assign unequivocally any NMR signals to these hydrogens at the working pH of 7.46. Previously these hydrogens had been assigned by default to the resonances lying between δ3.00 and δ3.50 in the ^{1}H NMR spectrum of the *para*-Hoechst/DNA complex. This spectral window does not normally contain any DNA hydrogen resonances. However, our studies of the *meta*-Hoechst/DNA complex show that this window actually contains resonances from shielded 5′ and 5″ hydrogens belonging to central T residues of the DNA. From a comparison of the 500-MHz *para*-Hoechst/DNA complex data and the 600-MHz *meta*-Hoechst/DNA complex data, it is clear that the assignments in this spectral window should be the same for both complexes. The assignment of these resonances occurs by correct identification of 4′ hydrogens

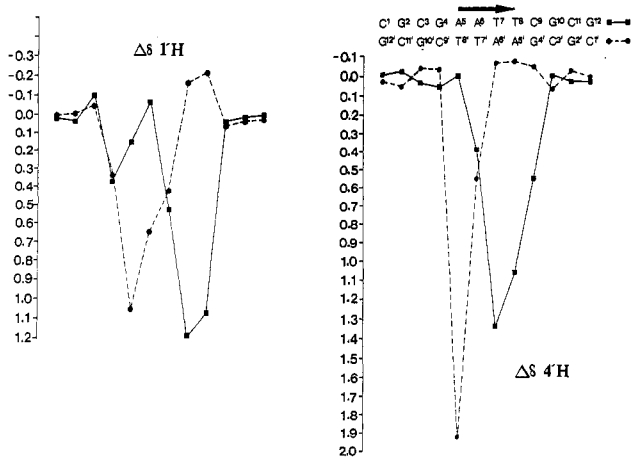

FIGURE 2: Plots illustrating the difference ($\Delta\delta$) in chemical shifts of the 1′ and 4′ sugar proton resonances between the *meta*-Hoechst-bound DNA and the free DNA. Positive shifts indicate that a paricular resonance becomes more shielded when the ligand is bound.

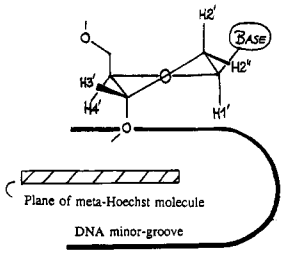

FIGURE 3: Representation of the minor groove of the *meta*-Hoechst/d(CGCGAATTCGCG)$_2$ complex in the region of the binding site showing how the H4′ protons of the sugar moieties overhang the aromatic rings of the benzimidazole groups of *meta*-Hoechst to a greater extent than the H1′ protons.

which resonate in the window normally reserved for 2′ and 2″ hydrogen resonances between approximately δ2.00 and δ3.00. The remarkable change in the chemical shift of the T$^{8'}$ 4′ hydrogen resonance by over 1.9 ppm to low frequency on binding of *meta*-Hoechst locates this hydrogen directly above one of the benzimidazole moieties of the ligand. Whilst it is known that the 1′ hydrogen resonances of DNA shift to low frequency on minor-groove binding of an aromatic ligand (Parkinson et al., 1990), recourse to a molecular model clearly shows that the 4′ hydrogens are likely to be far more influenced by magnetic anisotropy than the 1′ hydrogens. Chemical shift changes for the 1′ and 4′ hydrogen resonances in the *meta*-Hoechst/DNA complex are shown in Figure 2. The rationale behind these alterations is clear from part of the model of the complex shown in Figure 3.

Exchangeable Hydrogens. The exchangeable hydrogen resonances were assigned (Table 2) from the 175-ms mixing time NOESY data set acquired from a sample dissolved in 85% H_2O/15% D_2O. Aided by a one-dimensional NMR study of the complex in this solvent at various temperatures and pH values, it was possible to show that each of the GC base-paired imino hydrogens resonates at a distinct chemical shift. The AT base-paired imino hydrogens, on the other hand, do not have such distinct chemical shifts at the working pH of 7. Inspection of the 500-MHz spectrum of the *para*-Hoechst complex and its comparison with the 600-MHz spectrum of the *meta*-Hoechst complex at different pH values (Figure 4) revealed a marked difference between the two in this region of the NMR spectrum. There is a marked difference in the DNA proton resonances between the two complexes. The complete absence of a *meta*-Hoechst N1H proton resonance is curious. To investigate this further we carried out a pH-dependent NMR study from pH_{meas} 4.12 to 8.32 by the gradual addition of small aliquots of NaOD/D_2O. A number of resonances underwent pH-dependent changes in chemical shift (Figure 5).

Table 3: Intermolecular NOEs Observed between *meta*-Hoechst and d(CGCGAATTCGCG)$_2$ in Their 1:1 Complex[a]

ligand proton	DNA proton
MH1	
MH2	C^{9}5′H
MH4	T^{8}1′H, A^{5}2H, A$^{6'}$2H, A$^{6'}$1′H, T$^{7'}$1′H
MH6	G^{10}4′H
MH9	A$^{6'}$2H, T^{7}1′H, T$^{7'}$1′H, T^{8}1′H
MH11	
MH12	T$^{8'}$4′H, T^{8}4′H, T$^{8'}$5″H, T$^{8'}$5′H
MH16	A^{5}2H, A^{6}2H, A^{6}1′H, T^{7}1′H, T$^{8'}$1′H, T^{8}5″H, T^{7}4′H
MH18	T^{7}4′H, T^{8}5″H
MH19	T^{7}4′H, T^{8}5″H, T^{8}5′H, T$^{8'}$4′H
$MHCH_3$	A^{5}2H
MHN3H	A^{6}2H, A$^{6'}$2H

[a] The *meta*-Hoechst hydrogen atoms are labeled according to Chart 1. The two magnetically inequivalent DNA strands are distinguished by the prime.

Intermolecular NOEs

The assignment detailed in the preceding section identified 32 intermolecular proton–proton NOEs (Table 3, Figure 6). Seven of these NOEs are between the DNA C2 hydrogens on the floor of the minor groove and the concave edge of the ligand. One NOE between the ligand piperazine methyl hydrogen atoms and the DNA A^{5}C2 hydrogen atom locates one end of the binding site. A combination of the NOEs shown in Table 3 and the chemical shift changes outlined previously served as constraints in the determination of the structure of this complex in solution.

Of particular interest are the four NOEs between the *meta*-Hoechst MH4 hydrogen and the DNA and the absence of *meta*-Hoechst MH2 hydrogen to DNA NOEs. This is particularly important in deciding if the *meta*-Hoechst phenolic OH group contributes to the orientation of the ligand on DNA.

Variable-Temperature Studies

The value of $\Delta G^{\ddagger}$ was determined by means of coalescence (Lee et al., 1988; Leupin et al., 1986), using the four thymidine methyl resonances as markers. At room temperature the four distinct resonances appear at δ1.352 (T^7 methyl), δ1.435 (T^8 methyl), δ1.252 (T$^{7'}$ methyl), and δ1.410 (T$^{8'}$ methyl). A solution of the 1:1 complex was heated gradually in the NMR probe, and ^{1}H NMR spectra were recorded at suitable intervals. Line broadening and eventual coalescence of the methyl signals from T^7 and T$^{7'}$ and T^8 and T$^{8'}$ residues occurred as the complex entered fast exchange and the two strands of the oligonucleotide became equivalent. The chemical shift differences between the two sets of resonances (16.8 and 63.6 Hz at 600 MHz and 25 °C) gave rise to two different coalescence temperatures (340 and 352 K). Substitution of these values into eq 1 gave values of $\Delta G^{\ddagger}$ of 73.3 and 72.0 kJ mol^{-1}, respectively. These values are slightly higher than those for the complex of *para*-Hoechst with d(CGCGAATTCGCG)$_2$ (Parkinson et al., 1992).

$$\Delta G^{\ddagger} = 19.14 T_{coal}[9.95 + \log(T_{coal}/\Delta\delta)] \text{ J mol}^{-1} \quad (1)$$

Molecular Graphics

Distance Constraints. Interproton distance constraints between the oligonucleotide and *meta*-Hoechst were calculated

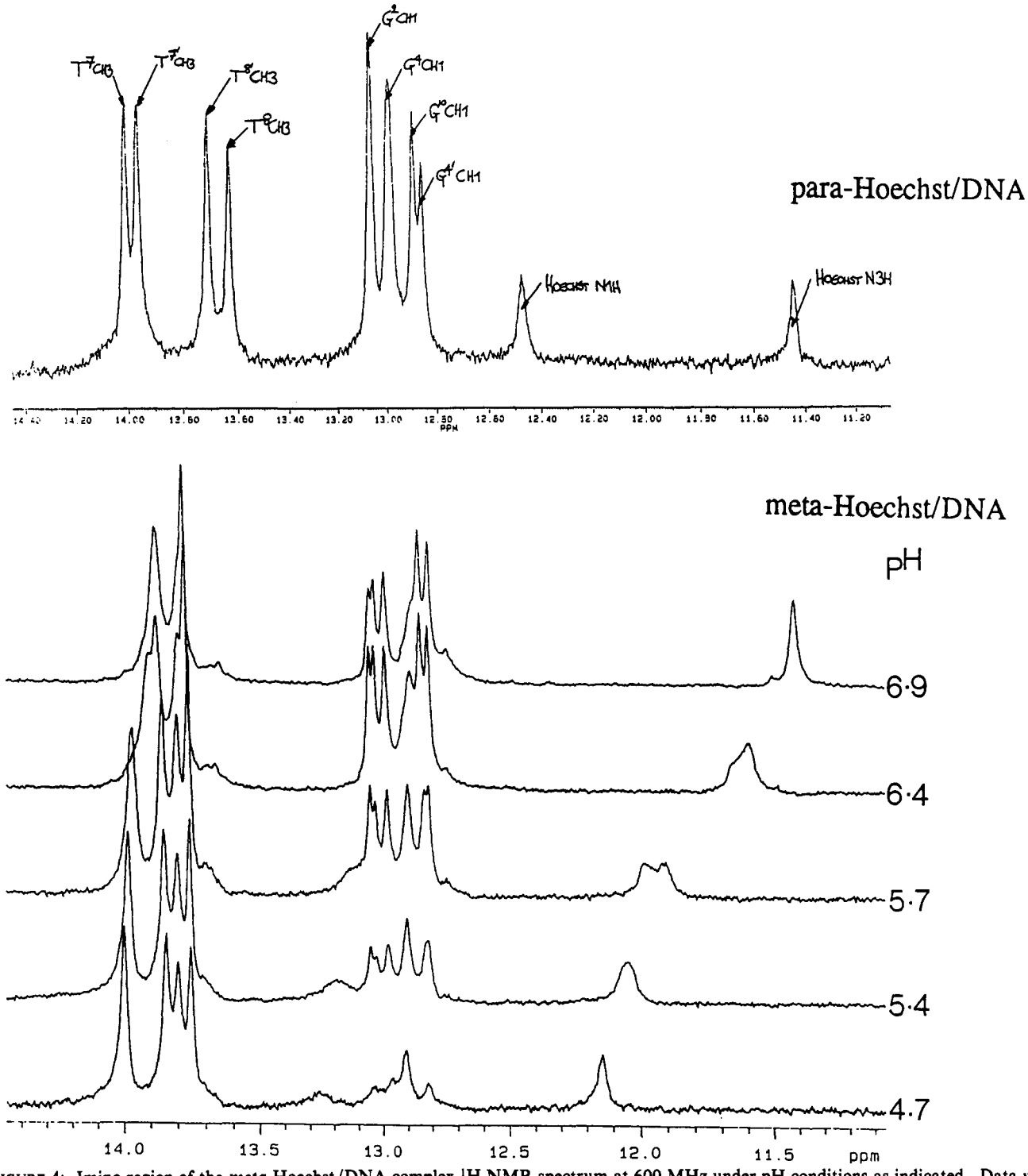

FIGURE 4: Imino region of the *meta*-Hoechst/DNA complex ^{1}H NMR spectrum at 600 MHz under pH conditions as indicated. Data was acquired using a NOESY pulse scheme incorporating a nonexcitation solvent suppression read pulse of the symmetrically shifted type. Data acquired in two dimensions at pH = 5.40 (not shown) enabled us to tentatively assign the broad resonance at 13.17 ppm to the O*H* of *meta*-Hoechst.

from NOE volume integral measurements, which were measured in NOESY data sets acquired consecutively at five different mixing times, recorded on a D_2O sample at 36 °C. Twenty-five intermolecular NOE volume integrals were measured together with a calibration NOE volume at each mixing time. Time development curves, plotted for all measured volumes, fell into two categories. Those curves resulting from plots of volume integral versus mixing time for the NOEs A$^{6'}$2H–MH9, A^{6}2H–MH16, and A$^{5'}$2H–MH4 together with C$^{9'}$(6H–5H) and C$^{11'}$(6H–5H) appeared typical of a direct NOE, little or not affected by spin diffusion (Piantini et al., 1982). C$^{9'}$(6H–5H) and C$^{11'}$(6H–5H) are used here for calibration, the distance between the 6 and 5 protons being 2.45 Å (Fede et al., 1991; Rance et al., 1983). The time development of the remaining NOEs between *meta*-Hoechst and the oligonucleotide was typical of NOEs *affected* by spin diffusion (Piantini et al., 1982).

The isolated spin-pair approximation (Bax & Davis, 1985; Kessler et al., 1989) was therefore used to calculate the three unknown distances A$^{6'}$2H–MH9, A^{6}2H–MH16, and A$^{5'}$2H–MH4. This approximation is only valid in certain special cases and as a general rule is invalid for bipolymers. For this

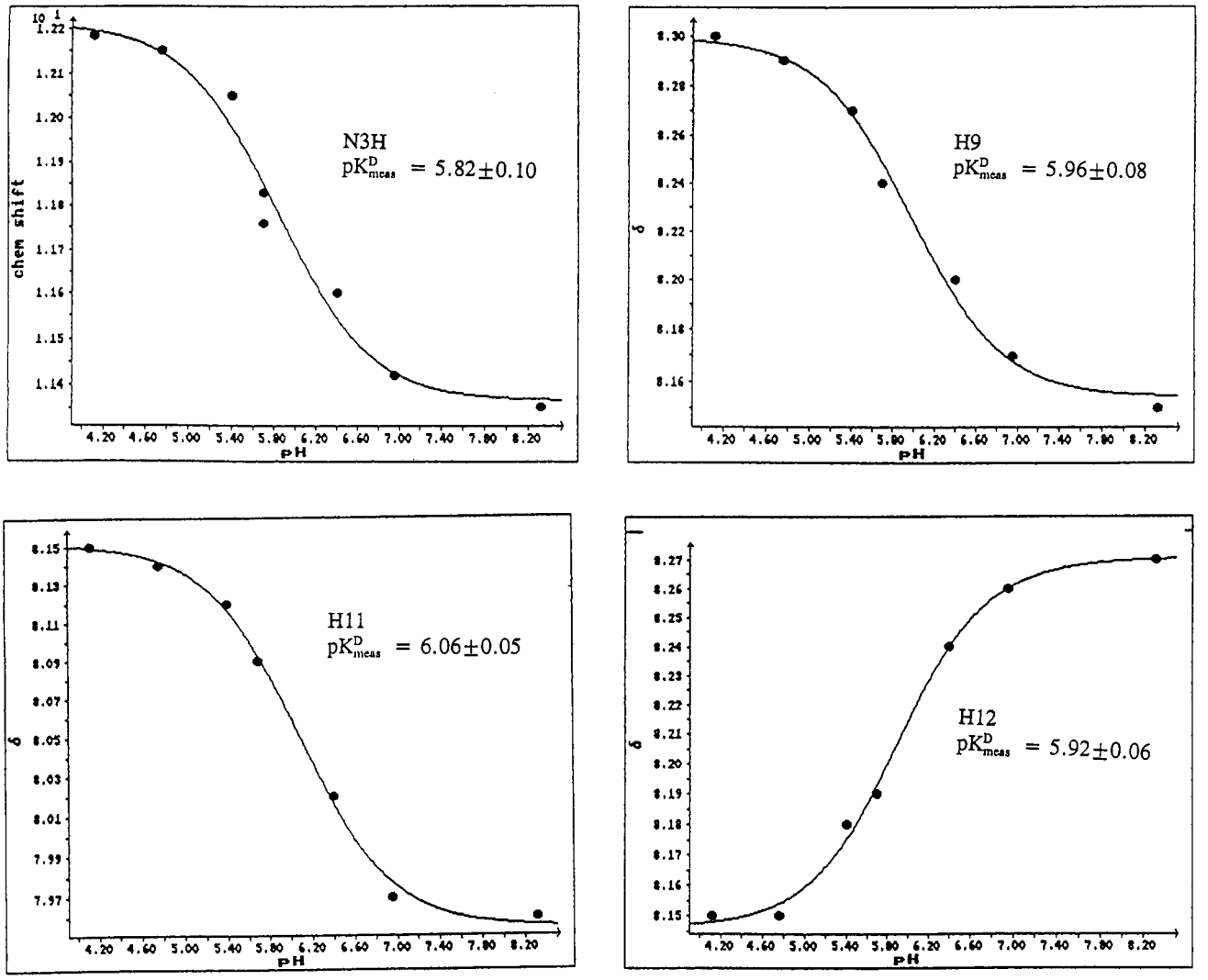

FIGURE 5: Profiles showing the pH dependencies of the chemical shifts of a number of resonances of bound Hoechst 33258 in D_2O media with the indicated pK_{meas} values.

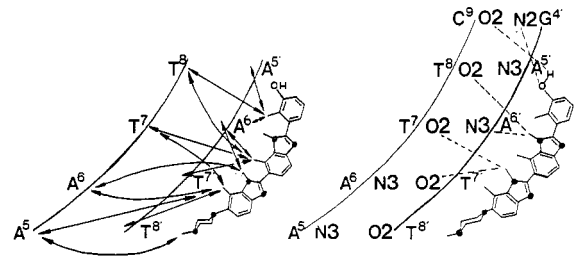

FIGURE 6: Illustration of the positions between which intermolecular proton–proton NOEs are observed (left) and the likely hydrogen-bonding network in the *meta*-Hoechst/DNA complex.

reason the remaining NOEs were not used to provide *calculated* distances. The isolated spin-pair approximation gives rise to the expression shown in eq 2

$$\frac{NOE_u}{NOE_c} = \frac{\sigma_u}{\sigma_c} = \frac{r_c^6 T_u}{r_u^6 T_c} \quad (2)$$

where u represents unknown, c represents calibration, NOE corresponds to the NOE volume integral, σ is the corresponding cross-relaxation rate, r is the interproton distance in Angstroms, and T is the molecular correlation or tumbling time. For a rigid molecule T_u and T_c cancel. Using this expression, the three unknown distances were calculated in a number of different ways, as shown in Table 4.

Table 4: Calculated NOE Distances between DNA and *meta*-Hoechst[a]

	$A^{6'}2H$–MH9 (Å)	$A^{6}2H$–MH16 (Å)	$A^{5'}2H$–MH4 (Å)
by initial rate	2.66	2.80	2.78
50-ms NOE volume	2.56	2.25	2.36
95-ms NOE volume	2.37	2.35	2.32
150-ms NOE volume	2.33	2.28	2.29
200-ms NOE volume	2.37	2.43	2.33
300-ms NOE volume	2.35	2.35	2.33

[a] Distances are averaged for data calculated from cross-peak volumes measured on both sides of the diagonal of NOESY data sets and also averaged on the basis of the use of different calibration cross-peaks.

The initial rate method (Table 4) is a measure of the initial rate of change of NOE intensity with time as the mixing time tends to zero. The actual NOE intensities at different mixing times were also used to calculate the unknown interproton distances. Due to interference from spin diffusion, distances calculated from NOESY data at long mixing times using eq 2 tend to be underdetermined (Piantini et al., 1982; Rance et al., 1983; Bax & Davis, 1985; Kessler et al., 1989). At short mixing times and for short distances when the NOE is less severely affected by spin diffusion, calculated distances are more precise relative to known distances. At short mixing times there is greater error in the calculation from poor signal to noise in the acquired data. We have therefore compared

the distances calculated on the basis of NOEs measured at all mixing times.

Given that a ±50% error in the measurement of an NOE intensity can result in a ±7% error in the calculated distance (Piantini et al., 1982) (±0.2 Å on a distance of 2.35 Å) the figures in Table 4 appear to be within acceptable error bounds. Thus we felt justified in using these three distances to triangulate more precisely the location of *meta*-Hoechst in the DNA minor groove. All other NOEs are severely affected by spin diffusion. However, their presence implies a loose upper bound distance constraint of 5 Å. Their inclusion in a more complete model based upon a full relaxation matrix approach is anticipated.

DISCUSSION

Previous studies of Hoechst 33258 have shown it to bind tightly to the AATT stretch of d(CGCGAATTCGCG)$_2$ and described in detail the three-dimensional structure of the 1:1 complex formed (Parkinson et al., 1990). The analogue described in the present study, *meta*-Hoechst (**2**), binds in a similar overall location.

Chemical shift differences between free and ligand-bound forms of the DNA are greatest in the central AATT stretch, grossly locating the binding site (Ebrahimi et al., 1992). As previously outlined, the 1′H and 4′H protons close to the central AATT region of the DNA see the most dramatic alterations in chemical shift. The identification of all the 4′H resonances completes the picture for the gross location of *meta*-Hoechst when bound to d(CGCGAATTCGCG)$_2$. Both 1′ and 4′ hydrogen atoms point into the minor groove of B-DNA structures. Figure 3 shows schematically how such hydrogens would become influenced by an aromatic ring approaching them as indicated. The change in chemical shift of the T^{8}′4⟹H resonance to low frequency (a result of diamagnetic anisotropy) by a larger amount than that of the T^{8}′1′H resonance shows that the benzimidazole moiety next to the piperazine ring is almost certainly located with the center of the six-membered aromatic ring located directly below the 4′H proton of the T^{8}′ residue (see Figure 3). Not only does this evidence unequivocally locate the dye in the DNA minor groove but it also determines that, as for the *para*-Hoechst complex (Parkinson et al., 1990), the *meta*-Hoechst dye binds to the central AATT region of the oligonucleotide. This is confirmed by the set of observed intermolecular NOEs. As in the previous study (Parkinson et al., 1990), chemical shift changes to low frequency also exist for some resonances from aromatic hydrogens located in the DNA major groove in the complex. This reports on some local DNA distortions (i.e. base-pair propellor-twist and roll) taking place in the major groove. This is interestingly commented upon by Fede et al. (1991). The 'titration' of the T-methyl resonances (Ebrahimi et al., 1992) indicates the 1:1 nature of the complex between **2** and d(CGCGAATTCGCG)$_2$. The replacement of two methyl signals each of an intensity corresponding to six hydrogen atoms (in the free oligonucleotide) by four methyl signals each of an intensity corresponding to three hydrogen atoms in the complex highlights the presence of four thymidine methyl signals from four bases having different chemical identities. The symmetry of the DNA is thus altered by the tight binding of the unsymmetrical ligand (**2**) in the minor groove. The fact that resonances are 'doubled' is evidence for a complex in slow exchange. As the temperature is raised, coalescence of doubled resonances occurs as the complex enters fast exchange. This evidence for a very tight complex is also backed up by NOE data. At 50 °C the NOEs A^{6}′2H–MH9, A^{6}-2H–MH16, and A^{5}′2H–MH4, between the recognition edge of the ligand **2** and the floor of the DNA minor groove, are still very strong.

As in the case of **1** bound to d(CGCGAATTCGCG)$_2$, the data for the current complex clearly point to a single binding site. Firstly, only one set of NMR resonances exist for the DNA-bound ligand. Whilst in theory the NMR spectrum of a DNA-bound ligand could be an average of the ligand in fast exchange, we know from the NMR spectrum of the ligand-bound DNA that the ligand is in slow exchange with its DNA binding site. Secondly the NOEs and chemical shift changes are only consistent with a single binding site. The presence of only one set of resonances for the bound ligand is interesting compared to the work of Fede et al. (Fede et al., 1991). They report the occurrence of two piperazine *N*-methyl resonances at 2.96 and 2.56 ppm in their study of **1** with d(GTGGAATTCCAC)$_2$. Their explanation for this is the presence of more than one piperazine ring conformation in the complex of **1** at the AATT binding site, putting the piperazine *N*-methyl group into more than one chemically distinct environment. In our study we see only a single piperazine *N*-methyl signal at 2.967 ppm at all temperatures used for the study. This is in agreement with our previous work on the complex of **1** with d(CGCGAATTCGCG)$_2$ (Parkinson et al., 1990). Fede et al. (Fede et al., 1991) also report chemical shift assignments for the piperazine methylene hydrogens at 4.34 and 3.40 ppm. They noted that the latter resonance was observed to be broad and made up of two components at 3.38 and 3.43 ppm. The presence of these two resonances was also ascribed to the existence of more than one piperazine ring conformation when **1** was bound to its DNA binding site. In our present study of **2** bound to d(CGCGAATTCGCG)$_2$ we have been unable to assign any resonances to the piperazine methylene protons. In our previous study (Parkinson et al., 1990) we suggested that the piperazine methylene protons resonated at between 3.00 and 3.70 ppm, a region of the spectrum normally devoid of DNA resonances. We wrongly assumed that any resonances appearing in this region of the spectrum must be due to the bound ligand. In the present study we have shown that DNA resonances can be extensively shifted to low frequency by the shielding effects of a bound ligand. We have observed a broad resonance at 3.38 ppm in our study. At elevated temperatures this resonance splits and sharpens into two resonances which we ascribe to C^{9}5″H at 3.395 ppm and T^{8}′5″H at 3.36 ppm. The fact that we cannot yet assign the piperazine methylene protons as Fede et al. (Fede et al., 1991) were able to do implies some difference between the two complexes. An underlying broad hump between 3.00 and 4.00 ppm in the present study could be due to the piperazine methylene protons. In this case the piperazine ring is indeed experiencing some conformational flexibility, as reported by Fede et al. (Fede et al., 1991), but at an intermediate rate compared to the NMR time scale, resulting in resonance broadening.

The overall similarity of the *meta*-Hoechst/DNA complex to the *para*-Hoechst/DNA complex is clear from the close correlation of the chemical shifts for the proton resonances in each case. Therefore, differences between the chemical shifts which do occur are worth noting. Two nonexchangeable adenine C2 hydrogen chemical shifts differ in particular between the *meta*- and *para*-Hoechst/DNA complexes, namely A^{6}C2H and A5′C2H. The higher frequency resonance of both of these hydrogens in the *meta*-Hoechst complex may indicate a closer approach of the ligand to the DNA when bound.

The 32 intermolecular NOEs identified (Table 3) served to locate the twisted molecule of **2** in the AATT minor groove. In Figure 6 are shown some of the intermolecular NOEs between the oligo and **2** (see Table 3) alongside the hydrogen-bonding network which is consistent with these. The main purpose of the present study was to test the hypothesis that hydrogen bonding could be designed in the Hoechst/DNA complex, and it is to this aspect that we turn in more detail. The first indication that such hydrogen bonding may indeed occur is in the absence of MH2 to DNA NOEs coupled with the observation of NOEs from the ligand MH4 proton to $T^8$1′H, $A^{5'}$2H, $A^{6'}$1′H, and $T^{7'}$1′H. Of these, the interactions of MH4 with $A^{6'}$1′H and $A^{5'}$2H are still readily observable at 50 °C when many other NOEs have disappeared. Thus, the orientation of the phenolic region of **2** in the minor groove (with the *m*-OH group directed into the minor groove) is quite resistant to temperature increase. In studies of the dynamics of **1** with d(CGCGAATTCGCG)$_2$, we found that Hoechst 33258 (**1**) binds with its bis-benzimidazole region localized securely in the minor groove but with its *para* phenolic group able to flip easily in the groove (Parkinson et al., 1992). Other workers found a similar rotational freedom for the *para* phenolic group of **1** in its 2:1 complex with d(CTTTTG-CAAAAG)$_2$ (Searle & Embrey, 1990) and its 1:1 complex with d(GGTAATTACC)$_2$ (Embrey et al., 1993).

Embrey et al. (1993) have shown that the rate of phenolic ring-flip in Hoechst 33258 complexed to d(GGTAATTACC)$_2$ is $>10^3$ s^{-1}, which is considerably greater than the rate predicted from the barrier in rotation based on a static DNA/ligand structure. They interpreted this to mean that there must be considerable fluctuation of local DNA conformation to allow ligand movement in this way. In the case of **2**, moving the OH group to the *meta* position seems to freeze this ring flipping. Not only therefore does this support a significant binding interaction (such as the dual hydrogen bond involving the *m*-OH and C=O of C^9 plus the NH_2 of $G^{4'}$) but it also indicates that this interaction is sufficient to prevent local DNA breathing in this region relative to the complex with **1**.

The coalescence studies of **1** (Parkinson et al., 1992) and **2** (this study) with d(CGCGAATTCGCG)$_2$ provide values of $\Delta G^{\ddagger}$ (measured using the two pairs of T-methyl resonances) of

$\Delta G^{\ddagger}$ for **1**	70 kJ mol^{-1} 69 kJ mol^{-1}	and	$\Delta G^{\ddagger}$ for **2**	73 kJ mol^{-1} 72 kJ mol^{-1}

The errors associated with $\Delta G^{\ddagger}$ values measured from coalescence studies are typically ±5 kJ mol^{-1} (Parkinson et al., 1992), so that it is not safe to assert that the 2–3 kJ mol^{-1} greater stability to exchange of the oligo complex of **2** compared to **1** is ascribable to such hydrogen bonding, but it is certainly consistent with it.

We were also able to detect at pH 5.4, 25 °C, a resonance at 13.17 ppm (see Figure 4 and Table 1) which could be tentatively assigned to the phenolic OH proton of **2**, at a chemical shift which is consistent with hydrogen bonding (to C=O or C=N). This resonance shows NOEs to MH4 (*ortho* to it) and to $A^{6'}$C2H, again consistent with the direction of the OH group into the minor groove.

pK_a of meta-Hoechst Bound to d(CGCGAATTCGCG)$_2$. The ionic state of **1** bound to DNA has been discussed previously (Parkinson et al., 1990), and we can now discuss the situation for *meta*-Hoechst from direct pK_a determination of the ligand in its complex with d(CGCGAATTCGCG)$_2$.

From Figure 5 the bound form of *meta*-Hoechst reflects an ionization of $pK^{D}_{meas} = 5.96$ (taking the mean of the measured pK^{D} values for N3H, H9, H11, H12, and H19). This was measured in 15% D_2O, and a pH meter correction for work in D_2O as opposed to H_2O media must be applied. This is carried out by means of the relationship $pD = pH_{meas} + 0.35$ (Chang & Douglas, 1980) for fully deuterated media. Hence, the measured pK^{D} for *meta*-Hoechst in its complex with d(CGCGAATTCGCG)$_2$ is approximately 6.02 in 15% D_2O (using a correction of +0.06). For an acid of $pK_a \sim 6$, on going from H_2O to D_2O the pK_a value increases by $\sim +0.5$ pK units (Bell & Kuhn, 1963), which means that the pK^{H} for the bound state of *meta*-Hoechst (in 85% H_2O/15% D_2O) would be approximately 6.1. It is not straightforward to measure the pK_a value of free Hoechst dyes by NMR, as the free ligand suffers from extensive pH-dependent spin diffusion. Thus an estimate of the pK_a of the free form of the ligand is required. Whilst the pK_a^{H} of benzimidazole at 25 °C is reported to be 5.58 (Lane & Quinlan, 1960) and 5.55 (Walba & Isensee, 1961), 2-phenylbenzimidazole has a somewhat lower pK^{H} of 5.23 (Walba & Isensee, 1961). This elevated value of pK^{H} for bound *meta*-Hoechst (6.1 *cf.* 5.2) may be either due to the poor approximation of the *meta*-Hoechst situation provided by 2-phenylbenzimidazole or because the ionizing group (in principle either N1H or N3H at this stage of the analysis) is located in the relatively hydrophobic cavity formed by occlusion of *meta*-Hoechst to the minor groove. The Hoechst 33258/DNA interface has been estimated to have a dielectric constant of ~20 D by fluorescence studies (Jin & Breslauer, 1988), which would lower the pK_a of a cationic acid such as a benzimidazolium ion, although the negative electrostatic potential of the minor groove would favor the binding of the benzimidazolium ion form(s) of Hoechst ligands. At physiological pH values of around neutrality, the *meta*-Hoechst ligand binds with the benzimidazole group containing N3H in its neutral form, indicating that the latter effect is not strong enough to dominate the pK_a of the bound ligand at these heterocyclic sites. The identification of N3H as the monitored pK_a follows. Protons at positions H9 and H11 are mesomerically linked to N3H in its protonated state, whilst H12 and H19 interact through the inductive effect, lying effectively *meta* to the N3H-containing substituent on their respective benzene rings. Thus, all the resonances (N3H, H9, H11, H12, H19) effectively report the pK_a of the N3H site.

The observation of NOEs to DNA from N3H (Table 3) indicates that N3H points into the minor groove. The observation of two sets of resonances (chemical exchange) for protonated and neutral forms of the benzimidazole ring containing N3 shows that the N3H is in slow exchange. This is in contrast with *meta*-Hoechst N1H, which we assume to be always in *fast* exchange (probably with the bulk solvent), as we could not determine a resonance for it. By contrast with the case of **2**, both N1H and N3H resonances are detectable for the complex of **1** with d(CGCGAATTCGCG)$_2$ (Parkinson et al., 1990). At this stage we are unable to explain this difference between **1** and **2**.

Molecular modeling in which the B-DNA structure was allowed to change to move concomitantly with that of the minor groove binder led to gross distortion of the relative locations of the DNA base pairs even with short runs (*e.g.* 250 iterations of ABNR). By holding the B-DNA atoms rigid, sizable movements of the ligand could be achieved without generating nonsense structures. On the basis of previous NMR and crystal structures, this approximation was within our NOE error limits.

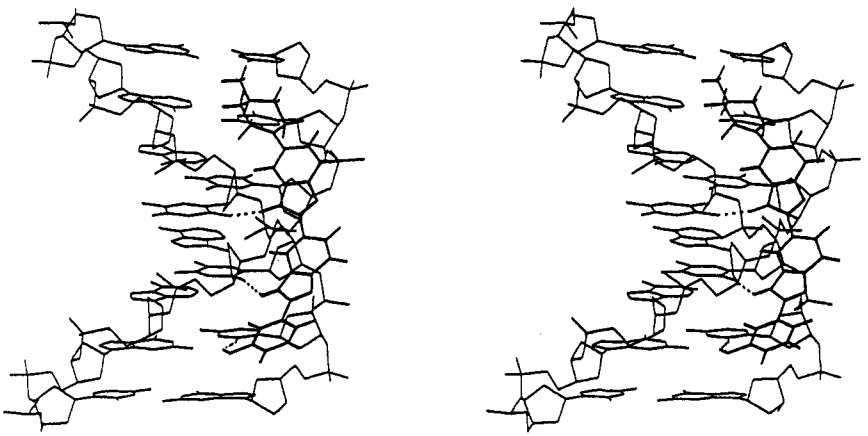

FIGURE 7: Stereo diagram showing the model of *meta*-Hoechst (bold) complexed with the B-DNA-configured d(CGCGAATTCGCG)$_2$. The location of the ligand was generated from the set of three precisely determined NOE distances. The ligand binds in a very similar fashion to the *p*-hydroxy analogue but with the *m*-hydroxy substituent directly H-bonding (dotted line) to the G$^{4'}$–C^{9} base pair (shown as the penultimate base pair from the bottom).

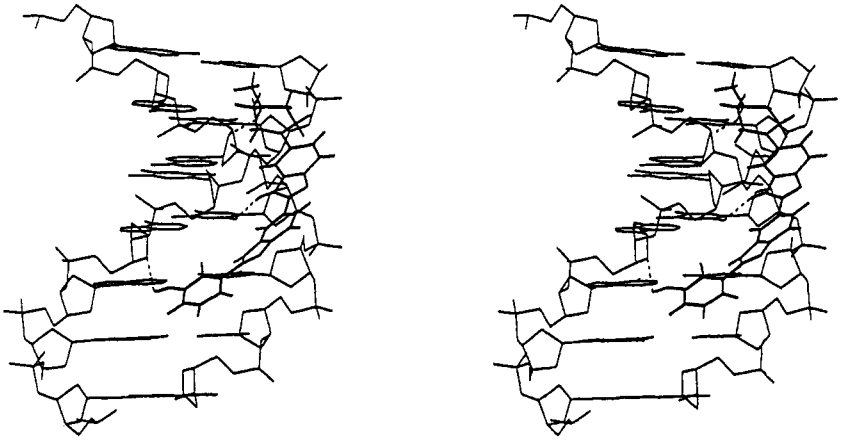

FIGURE 8: Stereo diagram of the model of *meta*-Hoechst (bold) complexed with d(CGCGAATTCGCG)$_2$ derived using the extended set of NOE distances. With the exception of the three precisely measured NOEs, the constraint distances were set to 4.0 Å. The additional constraints had the affect of shifting the ligand up to a base pair to put the phenolic group in direct juxtaposition to the A$^{6'}$–T^{7} base pair. The hydroxy substituent of *meta*-Hoechst can form a direct H-bond to the A$^{6'}$ O$^{4'}$ oxygen atom of the ribose ring (shown as a dotted line).

Figure 7 shows a stereo diagram of the model employing only the triple set of accurately determinable NOE distances. The *m*-hydroxyl group of the ligand can form direct H-bonds to the G$^{4'}$–C^{9} base pair, as initially predicted (Ebrahimi et al., 1992). Figure 8 shows the results of applying the extended set of NOE constraints with their approximated distances. During the first minimization (NOE and atomic constraints applied), the ligand shifted a full base pair 'upward' to place the phenolic group in line with the A$^{5'}$≡T^{8} basepair. Distortions of the ligand that resulted in this step were substantially relieved by the second minimization (with atomic but not NOE constraints applied). The third series of iterations (using both NOE and atomic constraints) resulted in much less ligand distortion. The final minimization allowed the ligand to relax back into a low-energy conformation. When the process was repeated with the ligand initially located at an alternative base pair above the final location (starting at A$^{6'}$=T^{7}), the final bound-ligand position was located at the median base pair (A$^{5'}$=T^{8}) in a substantially similar conformation. Here the *m*-hydroxy group could not H-bond to the C2 carbonyl of T^{8} but could H-bond to A$^{6'}$ O4′ (the cyclic oxygen of the ribose), where the *m*-hydroxyl group could be contained in the space between the C2 and N3 atoms of A$^{5'}$. The N1H proton could form a distorted H-bond with the C2 carbonyl of T^{8}, with N3H forming a H-bond with the C2 carbonyl of T^{7}. In this model an additional *o*-hydroxy group on the ligand could form a bidentate H-bond to the C2 carbonyl of T^{8}. This may serve to test these models; the choice of which is the more appropriate is difficult to assess because of the need to approximate the 29 NOE distances (necessary because of spin diffusion).

ACKNOWLEDGMENT

We are grateful (K.T.D.) to the SERC for a grant to use the NMR facilities at Edinburgh, to the Iranian Government (for support of SESE), and for a gift of d(CGCGAATTCGCG)$_2$ from the Oswell DNA Unit, Edinburgh.

REFERENCES

Bathini, Y., Rao, K. E., Shea, R. G., & Lown, J. W. (1990) *Chem. Res. Toxicol. 3*, 268.

Bax, A., & Davis, D. G. (1985) *J. Magn. Reson. 65*, 355.

Beerman, T. A., McHugh, M. M., Lown, J. W., Rao, S. R., & Bathini, Y. (1992) *Biochim. Biophys. Acta 113*, 53.

Bell, R. P., & Kuhn, A. T. (1963) *Trans. Faraday Soc. 59*, 1789.

Bontemps, J., Houssier, C., & Fredericq, E. (1975) *Nucleic Acids Res. 2*, 971.

Carrondo, M. A. A. F. de C. T., Coll, M., Aymami, J., Wang, A. H.-J., van der Marel, G. A., van Boom, J. H., & Rich, A. (1989) *Biochemistry 28*, 7849.

Chang, W. T., & Douglas, K. T. (1980) *Biochem. J. 187*, 843.

Comings, D. E. (1975) *Chromosoma 52*, 229.

Ebrahimi, S. E. S., Parkinson, J. A., Fox, K. T., McKie, J. H., Barber, J., & Douglas, K. T. (1992) *J. Chem. Soc., Chem. Commun.* 1398.
Embrey, K. J., Searle, M. S., & Craik, D. J. (1991) *J. Chem. Soc., Chem. Commun.* 1770.
Embrey, K. J., Searle, M. S., & Craik, D. J. (1993) *Eur. J. Biochem. 211*, 437.
Fede, A., Labhardt, A., Bannwarth, W., & Leupin, W. (1991) *Biochemistry 30*, 11377.
Goodsell, D., & Dickerson, R. E. (1986) *J. Med. Chem. 29*, 727.
Härd, T., Fan, P., & Kearns, D. R. (1990) *Photochem. Photobiol. 51*, 77.
Hare, D. R., Wemmer, D. E., Chou, S.-H., Drobny, G., & Reid, B. R. (1983) *J. Mol. Biol. 171*, 319.
Haworth, I. S., Burt, C., Gago, F., Reynolds, C. A., & Richards, W. G. (1991) *Anti-Cancer Drug Des. 6*, 59.
Jeener, J., Meier, B. H., Backmann, P., & Ernst, R. R. (1979) *J. Chem. Phys. 71*, 4546.
Jin, R., & Breslauer, K. J. (1988) *Proc. Natl. Acad. Sci. U.S.A. 85*, 8939.
Kessler, H., Griesinger, C., Kersebamm, R., Wagner, K., & Ernst, R. R. (1987) *J. Am. Chem. Soc. 109*, 607.
Kopka, M. L., Yoon, C., Goodsell, D., Pjura, P., & Dickerson, R. E. (1985) *Proc. Natl. Acad. Sci. U.S.A. 82*, 1376.
Kumar, S., Yadagiri, B., Zimmermann, J., Pon, R. T., & Lown, J. W. (1990) *J. Biomol. Struct. Dyn. 8*, 331.
Kumar, S., Joseph, T., Singh, M. P., Bathini, Y., & Lown, J. W. (1992) *J. Biomol. Struct. Dyn. 9*, 853.
Lane, T. J., & Quinlan, K. P. (1960) *J. Am. Chem. Soc. 82*, 2994.
Latt, S. A., & Stetten, G. (1976) *J. Histochem. Cytochem. 24*, 24.
Lee, M., Chang, D.-K., Hartley, J. A., Pon, R. T., Krowicki, K., & Lown, W. J. (1988) *Biochemistry 27*, 445.
Leupin, W., Chazin, W. J., Hyberts, S., Denny, W. A., & Wüthrich, K. (1986) *Biochemistry 25*, 5902.
Loontiens, F. G., Regenfuss, P., Zechal, A., Dumortier, L., & Clegg, R. M. (1990) *Biochemistry 29*, 9029.
Loontiens, F. G., McLaughlin, L. W., Diekmann, S., & Clegg, R. M. (1991) *Biochemistry 30*, 182.
Lown, J. W., Sim, S.-K., Majumdar, K. C., & Chang, R.-Y. (1977) *Biochem. Biophys. Res. Commun. 76*, 705.
Macura, S., Huang, Y., Suter, D., & Ernst, R. R. (1981) *J. Magn. Reson. 43*, 259.
Mikailor, M. V., Zasedateler, A. S., Krylov, A. S., & Gurskii, G. V. (1981) *Mol. Biol. (Moscow) 15*, 541.
Muller, W., & Gautier, F. (1975) *Eur. J. Biochem. 54*, 385.
Nagayama, K., Kumar, A., Wüthrich, K., & Ernst, R. R. (1980) *J. Magn. Reson. 40*, 321.
Parkinson, J. A., Barber, J., Douglas, K. T., Rosamund, J., & Sharples, D. (1990) *Biochemistry 29*, 10181.
Parkinson, J. A., Barber, J., Buckingham, B. A., Douglas, K. T., & Morris, G. A. (1992) *Magn. Reson. Chem. 30*, 1064.
Piantini, U., Sorensen, O. W., & Ernst, R. R. (1982) *J. Am. Chem. Soc. 104*, 6800.
Pjura, P. E., Grzeskowiak, K., & Dickerson, R. E. (1987) *J. Mol. Biol. 197*, 257.
Quintana, J. R., Lipanov, A. A., & Dickerson, R. E. (1991) *Biochemistry 30*, 10294.
Rance, M., Sorensen, O. W., Bodenhausen, G., Wagner, G., Ernst, R. R., & Wüthrich, K. (1983) *Biochem. Biophys. Res. Commun. 117*, 479.
Rao, K. E., & Lown, J. W. (1991) *Chem. Res. Toxicol. 4*, 661.
Rao, K. E., Shea, R. G., & Lown, J. W. (1990) *Anti-Cancer Drug Des. 5*, 3.
Searle, M. S., & Embrey, K. J. (1990) *Nucleic Acids Res. 18*, 3753.
Sing, M. P., Tomi, J., Surat, K., Bathini, Y., & Lown, J. W. (1992) *Chem. Res. Toxicol. 5*, 597.
Smith, P. J., Lacy, M., Debenham, P. G., & Watson, J. V. (1988) *Carcinogenesis 9*, 485.
Sriram, M., van der Marel, G. A., Roelen, H. L. P., van Boom, J. H., & Wang, A. H.-J. (1992) *EMBO J. 11*, 225.
States, D. J., Haberkorn, R. A., & Ruben, D. J. (1982) *J. Magn. Reson. 48*, 286.
Steiner, R. F., & Sternberg, H. (1979) *Arch. Biochem. Biophys. 197*, 580.
Teng, M.-K., Usman, N., Rederich, C. A., & Wang, A. H.-J. (1986) *Nucleic Acids Res. 16*, 2671.
Toulme, J. J., & Hélène, C. (1988) *Gene 72*, 51.
Walba, H., & Isensee, R. W. (1961) *J. Org. Chem. 26*, 2789.
Zimmer, C., & Wahnert, U. (1986) *Prog. Biophys. Mol. Biol. 47*, 31.